J Biochem Tech (2011) 3(2): 270-273
ISSN: 0974-2328

Parametric constraints on the dynamic behavior of immobilized enzyme kinetics in a microreactor

Pratap R Patnaik*

Received: 20 August 2011 / Received in revised form: 08 November 2011, Accepted: 08 November 2011, Published online: 25 January 2012,

Abstract

The observed kinetics of reactions catalyzed by immobilized enzymes in microreactors may differ from their kinetics in well-mixed solution-phase reactors. While the steady-state differences have been analyzed before, the time-dependent differences have not been explored. In the present study, therefore, an initial feasibility analysis has been conducted to identify permissible regions for the kinetic parameters for dynamics solutions to exist. For a reaction catalyzed by alkaline phosphatase, it has been shown that the choices of the values of three vital parameters are inter-related and restricted to certain nonlinear loci. These limits add to the limits imposed by thermodynamic requirements, and they are important in determining dynamic behavior.

Key words: Microreactor, immobilized enzyme, alkaline phosphatase, transport effects, dynamic behavior.

Introduction

Microreaction-based processes are emerging swiftly as a preferred technology for a variety of chemical, biological and medical applications. The speed and width of research and commercial potential in this area is evident from the large number of recent reviews (Matosevic et al. 2010; Miyazaki et al. 2008; Lin et al. 2009; Griffiths and Tawfik)2011) and the observation that the world-wide market for microfluidic technologies was about £1.98 billion in 2008, with a projected increase of 15% every year (Mindbranch 2010). These encouraging data are strengthened by the large number of patents (Hessel et al. 2008) and commercial processes (Dolomite 2010; Microfluidics 2010) pertaining to microreactions.

The rapid growth of microfluidic processes may be attributed to their many advantages. They are less costly than conventional processes, more efficient, and have greater reproducibility. Since the reactions are carried out in long narrow tubes, the ratio of surface area to volume is large, thereby enabling efficient heat dissipation and accurate control (Hessel and Lowe 2010; Haeberle and Zengerle 2007) of temperature. This advantage makes microreactors effective for highly exothermic reactions, as in Fischer-Tropsch synthesis (Guettel et al. 2008) and steam reforming of methane/ methanol (Arzamendi et al. 2009).

The ability to implement sophisticate controls, often through microelectronic manufacturing systems technologies, the absence of turbulent mixing, and the low volumes of production (compared to chemical and petrochemical processes) favor the use of integrated microreactors for biological processes generating high-value products. Many of these processes are catalyzed by cells or enzymes, and therefore enzymatic microreactors have been the subject of expanding research. These reactors have been employed for protein and peptide mapping (Palm and Novotny 2004), combinatorial synthesis (Watts 2005), DNA analyses (Paegel et al. 2003) and immunoassays (Ohno et al. 2008).

Recent advances in integrating microreactors with analytical devices have accelerated their analytic and kinetic applications. Analytic applications, especially micrototal analysis systems, have been employed for many systems and are discussed elsewhere (Kim and Park 2005; Ohno et al. 2008). The present study is in the area of kinetic applications, which are of more recent origin but are equally important as discussed below. Determination of reaction kinetics in enzymatic microreactors, especially those utilizing immobilized enzymes, is important because the predominantly laminar flow makes diffusional and mass transfer resistances more significant than in larger well-mixed reactors (McMullen and Jensen 2010). In addition, owing to the complex interactions among several microdevices on a single chip and the complex channel designs sometimes needed, kinetics in microreactors may be more sensitive to perturbations than they are in macroscale reactors.

The three dimensional structure of the Defensin DM-AMP1 is not reported to have been resolved. In the present study, a computational approach is used to predict the three dimensional structure of the DMAMP1 by homology modelling. The approach

Pratap R. Patnaik

Department of Chemical Engineering, C. V. Raman College of Engineering, Bidyanagar, Mahura, Janla, Bhubaneswar-752054, Odisha

Tel: 09040930337; Fax: 0674-2113593
E-mail: pratap.r.patnaik@gmail.com

produces the valid structural model with the available template which having suitable amino acid identity.

Enzyme Kinetics in Microreactors

The stronger diffusion control and the larger surface-to-volume ratios of microreactors imply that the observed kinetics in these reactors may differ from those in larger conventional reactors. Recognizing this, many in investigators have specifically addressed enzyme kinetics in microreactors.

Mao et al. (2002) studied the kinetics of alkaline phosphatase (AP) immobilized in a microchannel under no flow conditions. While the Michaelis-Menten constant, K_m, was close to its solution-phase value, the turn-over rate, k_{cat}, was six times smaller. Seong et al. (2003) had similar observations for horseradish peroxidase and β-galactopyranoside, both immobilized in continuous-flow packed-bed reactors. Their K_m value was obtained by extrapolating their data to a zero-flow condition; if so, the agreement between the immobilized and the solution-phase values of K_m is puzzling because increases in flow should reduce mass transfer resistance and thus change the observed K_m (Kerby et al. 2006). Moreover, Seong et al.'s results contradict those reported by Lilly et al. (1968) for the hydrolysis of benzoylarginine ethyl ester. Lilly and coworkers observed a decrease in K_m with increasing flow rate of the substrate. Contrary to Seong et al., Lilli et al. extrapolated their data to large flow rates, arguing that this minimized mass-transfer resistance.

The kinetics of immobilized AP were also studied by Gleason and Carbeck (2004) and by Koh and Pishko (2005). The former authors conducted their experiments at a sufficiently high flow rate to eliminate the diffusion boundary layer and observed K_m values close to those in solution-phase kinetics but much smaller k_{cat} values, similar to Mao et al. (2002). Koh and Pishko (2005), however, did not minimize diffusion resistance and obtained much smaller values of K_m.

These results might suggest that the presence of mass transfer resistance is a likely reason for immobilized enzyme kinetics in microreactors being different from those in solution-phase. However, in a recent study Kerby et al. (2006) have argued against this explanation. Using the AP system for comparison with earlier studies, they hypothesized that occupation of active enzyme sites by intermediates and product molecules alters the intrinsic kinetics itself, regardless of diffusion and mass transfer effects. Since this phenomenon is not involved in solution-phase kinetics, the apparent values of k_{cat} and K_m differ between the two systems. The higher the conversion, the greater is the degree of occupation of active sites by molecules other than the substrate (s), and correspondingly the two sets of kinetic parameters also differ more.

On this basis, Kerby et al. (2006) modified the Michaelis-Menten kinetics for AP to enable it to be valid over a wide range of conversions. Their model is described below and used for further analysis.

Kinetics of Alkaline phosphatase (AP)

Kerby et al. (2006) began with the assumption that AP–catalyzed reactions follow Michaelis-Menten kinetics according to the mechanism

$$A + E \underset{\alpha_1}{\overset{\beta_1}{\rightleftharpoons}} AE \overset{\beta 2}{\rightarrow} E + B + P \quad (1)$$

Here A is the substrate, E the enzyme AP, and B and P are products.

For a differential packed bed, as in a packed microchannel, mole balance with Michaelis-Menten kinetics at steady state yields

$$u\frac{dc_A^b}{dz} = -\frac{v_{max}c_A^b}{K_m + c_A^b} \quad (2)$$

Eq. (2) may be integrated over the length, L, of the reactor to obtain

$$K_m \ln\frac{c_{AL}^b}{c_{A0}^b} + c_{AL}^b - c_{A0}^b = -\frac{v_{max}V_R}{Q} \quad (3)$$

To test the validity of Eq. (3), Kerby et al. applied it to the dephosphorylation of 6,8-difluoro-4-methylumbelliferyl phosphate (DiFMUp) by AP to 6,8-difluoro-4-methyl umbelliferone (DiFMU). Thus, in the model presented above, A is DiFMUp , B is DiFMU, P is $PO_4^{-2}$and E is AP.The microreactor was operated over a full range of conversions, from low to complete conversion. While Eq. (3) provided an accurate description at low conversions, it was inadequate at high conversions. The latter inadequacy was attributed to the occupation of a significant number of active sites by phosphate molecules, which the classic Michaelis-Menten formalism ignores. So Kerby et al. (2006) proposed an alternate model derived from a mechanism proposed earlier (Labow et al. 1993):

$$A + E \underset{\alpha_1}{\overset{\beta_1}{\rightleftharpoons}} AE \overset{\beta_2}{\rightarrow} EP + B \quad (4a)$$

$$EP \underset{\alpha_3}{\overset{\beta_3}{\rightleftharpoons}} E + P \quad (4b)$$

Considering the rates of adsorption and desorption of substrate molecules to be proportional to the number of unoccupied and occupied enzyme sites respectively, the dynamics of the concentration of occupied site was derived to be

$$\frac{dG_A}{dt} = \beta_1(G_\infty - G_A - G_P)c_A^b - (\alpha_1 + \beta_2)G_A \quad (5)$$

The adsorption/ desorption kinetics of PO_4^{-2} site may be described similarly as

$$\frac{dG_P}{dt} = \beta_2 G_A + \alpha_3(G_\infty - G_A - G_P)c_P^b - \beta_3 G_P \quad (6)$$

From Eqs. (5) and(6), Kerby et al. (2006) derived the steady state behavior of the microreactor. However, our focus here is on the dynamics. Hence we retain Eqs. (5) and (6), and divide each by G_∞ to obtain

$$\frac{dg_A}{dt} = \beta_1^*(1 - g_A - g_P) - (\alpha_1 + \beta_2)g_A \quad (7)$$

$$\frac{dg_P}{dt} = \beta_2 g_A + \alpha_3 c_P^b(1 - g_A - g_P) - \beta_3 g_P \quad (8)$$

where $\beta_1^* = \beta_1 C_A^b$.

Results and Discussion

Even though Kerby et al. (2006) acknowledge that their model still has weaknesses, it is more realistic than the Michaelis-Menten model used by other investigators (Mao et al. 2002; Gleason and Carbeck 2004; Koh and Pishko 2005). Moreover, Kerby et al.'s model applies to high conversions of the substrate, as required for an economically viable process. Under these conditions, a

significant proportion of PO_4^{-2} ions are bound to active sites on the immobilized enzyme matrix. Since there is no inflow of phosphate, unlike the substrate, the presence of a large concentration of bound PO_4^{-2} implies that their concentration in the bulk phase is small (relative to that of the substrate). This observation leads to the reasonable assumption that $c_P^b \ll 1$. Profitability of the process is also favored by conditions that shift the equilibrium between bound and free product in the direction of the latter, thereby also releasing more of the equilibrium. Mathematically this shift in the equilibrium may be expressed as $\alpha_3 \ll \beta_3$

These two simplifying assumptions allow the term $\alpha_3 C_P^b(1 - g_A - g_P)$ to be neglected in Eq. (8). Then Eqs. (7) and (8) may be written compactly as

$$\frac{d\bar{g}}{dt} = \bar{\bar{A}}\,\bar{g} + \bar{b} \qquad (9)$$

where $\bar{\bar{A}} = \begin{bmatrix} -(\beta_1^* + \alpha_1 + \beta_2) & -\beta_1^* \\ \beta_2 & -\beta_3 \end{bmatrix}$, $\bar{b} = [\beta_1^* \ 0]^T$ and $\bar{g} = [g_A \ g_P]^T$.

The superscript T denotes the transpose.

Eq. (9) may have one or two real solutions or a pair of complex conjugate solutions, depending on the sign of the discriminant

$$D \underline{\Delta} (\beta_1^* + \alpha_1 + \beta_2 + \beta_3)^2 - 4[(\beta_1^* + \alpha_1 + \beta_2)\beta_3 + \beta_1^* \beta_2] \qquad (10)$$

Accordingly, the temporal variation of $\bar{g}$ may be one of three types:

(i) D=O: $\bar{g}^T = C_1 \bar{k}^T e^{\lambda t} + C_2(\bar{k}^T t e^{\lambda t} + \bar{\varphi}^T e^{\lambda t})$ (11)

where φ is any solution of $[\bar{\bar{A}} - \lambda \bar{\bar{I}}]\bar{\varphi} = \bar{k}$, and λ is the single (real) root (eigenvalue) of Eq. (10). C_1 and C_2 are arbitrary constants.

(ii) $D > 0$: Let λ_1 and λ_2 be the two real unequal roots.

Then $\bar{g}^T = C_1 \bar{k}_1^T e^{\lambda_1 t} + C_2 \bar{k}_2^T e^{\lambda_2 t}$ (12)

In Eqs. (11) and (12), $\bar{k}$, $\bar{k_1}$ and $\bar{k_2}$ are the eigenvectors corresponding to λ, λ_1 and λ_3 respectively.

(iii) $D < 0$: We have a pair of complex conjugate roots, which may be denoted as $\lambda_1, \lambda_2 = \omega \pm \mu i$. The solution is then

$$\bar{g}^T = C_1 \bar{k}_1^T e^{\omega t}[a\cos(\mu t) - b\sin(\mu t)] + C_2 \bar{k}_2^T e^{\omega t}[a\sin(\mu t) + b\cos(\mu t)] \qquad (13)$$

where a and b are arbitrary constants.

Since D = O defines the locus that separates three regions of different dynamic behavior of the concentration vector $\bar{g}$, we analyze this further.

Let $\delta = \beta_1^* + \alpha_1 + \beta_2$; then $D = 0$ may be expanded to

$$(\delta + \beta_3)^2 - 4[\delta\beta_3 + \beta_1^*\beta_2] = 0 \qquad (14)$$

The roots this equation are

$$\beta_3 = \delta \pm 2\sqrt{\beta_1^*\beta_2} = \beta_1^* + \alpha_1 + \beta_2 \pm 2\sqrt{\beta_1^*\beta_2} \qquad (15)$$

From the first and second partial derivatives of β_3 with respect to β_1^* and β_2, it may be inferred that $\beta_3$increases with both β_1^* and β_2. However, the (nonlinear) variation may be of either of two types:

(i) Concave downward if $\beta_1^{*1/2}\,\beta_2^{-3/2} > 4$ (16)

(ii) Concave upward if $\beta_1^{*1/2}\,\beta_2^{-3/2} < 4$ (17)

These variations are portrayed graphically in Fig. 1; they define loci on which the parameters must lie in order to obtain a feasible solution for $\bar{g}$. For each set of values $(\beta_1^*, \beta_2, \beta_3)$ on these loci, the variation of $\bar{g}$ with time may be of one of the forms specified in Eqs. (11), (12) and (13), depending on the value of D. The present analysis shows that the permissible choices of β_1^*, β_2 and β_3 are inter-related and constrained by Eq. (15). When either β_1^* or β_2 is zero, both pairs of loci converge to unique but different values of β_3, as shown in Figure 1.

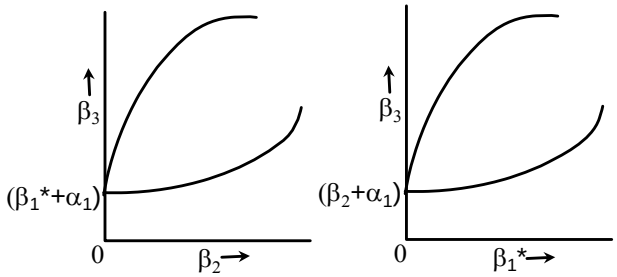

Figure 1. Loci of feasible choices for the parameters β_1^*, β_2 and β_3. Upper plots are for $\beta_1^{*1/2}\beta_2^{-3/2} > 4$ and lower plots for $\beta_1^{*1/2}\beta_2^{-3/2} < 4$. See text for details.

Conclusion

Owing to differences in hydrodynamics and transport limitations, the kinetics of chemical and biological reactions in microreactors may differ from those in larger, microreaction kinetics separately. Since most of these studies address the steady state behavior, a model proposed recently for a reaction catalyzed by immobilized alkaline phosphatase was analyzed qualitatively for the feasibility and time-dependent nature of its dynamic behavior. It was seen that feasible behavior is possible only on loci connecting three kinetic parameters, and the nature of the variation of the two key concentrations depends on the choice of values for these parameters. These constraints are not revealed by a steady state analysis, and they apply in addition to those imposed by thermodynamics.

Nomenclature

c_A^b	concentration of A in the bulk phase
c_{A0}^b	initial value of c_A^b
G_∞	total concentration of active sites on the enzyme
G_A	concentration of active sites occupied by A
G_P	concentration of active sites occupied by P
g_A	dimensionless G_A (=G_A/G_∞)
g_P	dimensionless G_P (=G_P/G_∞)

K_m Michaelis-Menten equilibrium constant
L total length of the microreactor
Q flow rate through the microreactor
t time
u fluid velocity through the microreactor
v_{max} maximum rate of reaction
V_R volume of the microreactor
z distance along the microreactor
α_1, α_3, β_1, β_2, β_3 kinetic parameters

References

Arzamendi G, Dieguez M, Montes M, Centeno A, Odriozola JA, Gandia LM (2009) Integration of methanol steam reforming and combustion in a microchannel reactor for H_2 production: A CFD simulation study. Catal Today 143: 25-31

Dolomite Microfluidics (2010) http://www.dolomite-microfluidics.com

Griffiths AD, Tawfik DS (2011) Miniaturizing the laboratory in emulsion droplets. Trends Biotechnol (in press)

Gleason NJ, Carbeck JD (2004) Measurement of enzyme kinetics using microscale steady state kinetic analysis. Langmuir 20: 6374-6381

Haeberle S, Zengerle R (2007) Microfluidic platforms for lab-on-a chip applications. Lab Chip 7: 1094-1110

Hessel V, Knobloch C, Lowe H (2008) Review on patents in microreactor and micropocess engineering. Recent Patents Chem Eng 1: 1-16

Hessel V, Lowe H (2010) Microreactor technology: Applications in pharma/chemical processing. Innov Pharma Technol 2: 88-92.

Guettel R, Kunz U, Turek T (2008) Fisher-Tropsch synthesis in monolithic honeycomb reactors. Chem Eng Technol 31: 746-754

Kerby MB, Legge RS, Tripathi A (2006) Measurements of kinetic parameters in a microfluidic reactor. Analyt Chem 78: 8273-8280

Kim KS, Park J-K (2005) Magnetic force-based multiplexed immunoassay using superparamagnetic nanoparticles in microfluidic channel. Lab Chip 5: 657-664

Koh WG, Pishko M (2005) Immobilization of multi-enzyme microreactors inside microfluidic devices. Sensors Actuators B 106 : 335-342

Labow BI, Herschlag D, Jencks WP (1993) Catalysis of the hydrolysis of phosphorylated pyridines by alkaline phosphatase. Biochemistry 32: 8737-8741

Lilly MD, Hornby WE, Crook EM (1968) Some changes in the reactivity of enzymes resulting from their chemical attachment to water-insoluble derivatives of cellulose. Biochem J 102: 669-674

Lin W-Y, Wang Y, Wang S, Tseng H-R (2009) Integrated microfluidic reactors. Nano Today 4: 470-481

Mao H, Yang T, Cremer PS (2002) Design and characterization of immobilized enzymes in microfluidic systems. Analyt Chem 74: 379-385

Matosevic S, Szita N, Baganz F (2010) Fundamentals and applications of immobilized microfluidic enzymatic reactors. J Chem Technol Biotechnol 86: 325-334

McMullen JP, Jensen KF (2010) Integrated microreactors for reaction automation: new approaches to reaction development. Ann Revs Analyt Chem 3: 19-42

Microfluidics Corporation (2010) Available via link http://www.microfluidicscorp.com

Mindbranch, Microfluidic Technologies (2010) Available via link http://www.mindbranch.com/Microfluidics-Technologies-R2-768

Miyazaki M, Honda T, Yamaguchi H, Briones MPP, Maeda H (2008) Enzymatic processing in microfluidic reactors. Biotechnol Genet Eng Revs 25: 405-428

Ohno K, Tachikawa K, Manz A (2008) Microfluidics: Applications for analytical purposes in chemistry and biochemistry. Electrophoresis 29: 4443-4453

Paegel BM, Blazej RG, Mathies RA (2003) Microfluidic devices for DNA sequencing: Sample preparation and electrophoretic analysis. Curr Opin Biotechnol 14: 42-50

Palm AK, Novotny MV (2004) Analytical characterization of a facile porous polymer moinolithic trypsin microreactor enabling peptide mass mapping using mass spectrometry. Rapid Commun Mass Spectrom 18: 1374-1382

Seong GH, Heo J, Crooks RM (2003) Measurement of enzyme kinetics using a continuous-flow microfluidic system. Analyt Chem 75: 3161-3167

Watts P (2005) The application of microreactors in combinatorial chemistry. QSAR Combin Sci 24: 701-711